forests

MDPI

Article

Risk Assessment of Carbon Stock Loss in Chinese Forests Due to Pine Wood Nematode Invasion

Shaoxiong Xu [1,2], Wenjiang Huang [1,2,*], Dacheng Wang [2], Biyao Zhang [2,3], Hong Sun [4], Jiayu Yan [4], Jianli Ding [1] and Xu Ma [1]

[1] College of Geography and Remote Sensing Sciences, Xinjiang University, Urumqi 830046, China; sx_xu@xju.edu.cn (S.X.); maxu2020@xju.edu.cn (X.M.); dingjl@xju.edu.cn (J.D.)
[2] Key Laboratory of Remote Sensing and Digital Earth, Aerospace Information Research Institute, Chinese Academy of Sciences, Beijing 100101, China; wangdc@aircas.ac.cn (D.W.); zhangby@aircas.ac.cn (B.Z.)
[3] Key Laboratory of Earth Observation of Hainan Province, Hainan Aerospace Information Research Institute, Sanya 572029, China
[4] Key Laboratory of National Forestry and Grassland Administration on Forest and Grassland Pest Monitoring and Warning, Center for Biological Disaster Prevention and Control of National Forestry and Grassland Administration, Shenyang 110034, China; sunhongcaf@163.com (H.S.); yanjiayu212@163.com (J.Y.)
* Correspondence: huangwj@aircas.ac.cn; Tel.: +86-138-1189-0218

Abstract: Chinese forests, particularly the coniferous forest ecosystems represented by pines, play a crucial role in the global carbon cycle, significantly contributing to mitigating climate change, regulating regional climates, and maintaining ecological balance. However, *pine wilt disease* (PWD), caused by the *pine wood nematode* (PWN), has become a major threat to forest carbon stocks in China. This study evaluates the impact of PWN invasion on forest carbon stocks in China using multi-source data and an optimized MaxEnt model, and the study analyzes this invasion's spread trends and potential risk areas. The results show that the high-suitability area for PWN has expanded from 68,000 km^2 in 2002 to 184,000 km^2 in 2021, with the spread of PWN accelerating, especially under warm and humid climate conditions and due to human activities. China's forest carbon stocks increased from 111.34 billion tons of carbon (tC) to 168.05 billion tC, but the carbon risk due to PWN invasion also increased from 87 million tC to 99 million tC, highlighting the ongoing threat to the carbon storage capacity. The study further reveals significant differences in tree species' sensitivity to PWN, with highly sensitive species such as Masson's pine and black pine mainly concentrated in the southeastern coastal regions, while less sensitive species such as white pine and larch show stronger resistance in the northern and southwestern areas. This finding highlights the vulnerability of high-sensitivity tree species to PWN, especially in high-risk areas such as Guangdong, Guangxi, and Guizhou, where urgent and effective control measures are needed to reduce carbon stock losses. To address this challenge, the study recommends strengthening monitoring in high-risk areas and proposes specific measures to improve forest management and policy interventions, including promoting cross-regional joint control, enhancing early warning systems, and utilizing biological control measures, while encouraging local governments and communities to actively participate. By strengthening collaboration and implementing control measures, the health and sustainable development of forest ecosystems can be ensured, safeguarding the forests' important role in climate regulation and carbon sequestration and contributing to global climate change mitigation.

Keywords: pine wood nematode; MaxEnt model; PWN-sensitive tree species; forest carbon stock risk

check for updates

Academic Editor: Viacheslav I. Kharuk

Received: 12 January 2025
Revised: 2 February 2025
Accepted: 4 February 2025
Published: 11 February 2025

Citation: Xu, S.; Huang, W.; Wang, D.; Zhang, B.; Sun, H.; Yan, J.; Ding, J.; Ma, X. Risk Assessment of Carbon Stock Loss in Chinese Forests Due to Pine Wood Nematode Invasion. *Forests* **2025**, *16*, 315. https://doi.org/10.3390/f16020315

Copyright: © 2025 by the authors. Licensee MDPI, Basel, Switzerland. This article is an open access article distributed under the terms and conditions of the Creative Commons Attribution (CC BY) license (https://creativecommons.org/licenses/by/4.0/).

1. Introduction

China, as one of the countries with the richest forest resources in the world, plays a crucial role in maintaining the global carbon cycle and ecological balance through its forest ecosystems [1,2]. Forests fix carbon dioxide from the atmosphere into carbon through photosynthesis, providing essential support for achieving global carbon neutrality goals [3,4]. However, forest ecosystems face multiple threats, among which pine wood nematode disease (PWD) has become one of the key factors affecting forest carbon stocks. PWD not only directly causes the death of pine trees but also accelerates carbon release, weakening the role of forests as carbon sinks and thus having a severe impact on the forest carbon balance [5].

Traditional studies on the forest carbon loss caused by pests have primarily focused on estimating the impact of pest outbreaks on the carbon cycle using forest inventory data and model simulations. These studies often emphasize tree mortality, biomass reduction, and the weakening of forests' carbon sink capacity due to pest outbreaks. For example, Kurz et al. (2008), based on monitoring data from Canadian forests, found that natural disturbances (including pest outbreaks and wildfires) could transform affected forests from carbon sinks to carbon sources, with the future carbon sink capacity showing high uncertainty [6]. Similarly, Liu et al. (2011) demonstrated that, in temperate forests, tree mortality caused by insect outbreaks significantly reduced carbon sequestration, thereby weakening the role of forest ecosystems as carbon sinks [7]. In addition, Quirion et al. (2021), using data from the U.S. Forest Inventory and Analysis (FIA) program, reported that carbon accumulation decreased by 69% in plots affected by pests and by 28% in plots affected by diseases, resulting in an annual carbon loss of approximately 12.83 Tg [8]. These studies have quantitatively highlighted the significant impacts of pest and disease disturbances on forest carbon sinks. In terms of research methods, Bright et al. (2012) employed LiDAR and multispectral imaging technology to assess the effects of mountain pine beetles on aboveground carbon stocks in Idaho's forests. Their findings revealed that pest outbreaks significantly reduced biomass and carbon stocks [9]. In China, Gao et al. (2018) conducted a study on pine wilt disease (PWD) in the Three Gorges Reservoir area, showing that forest biomass, carbon stocks, and nitrogen stocks experienced significant dynamic changes following pest invasion, especially during the early stages [10].

Pest outbreaks not only directly lead to rapid carbon release through tree mortality but may also exacerbate carbon stock loss through indirect pathways. For example, studies by Kurz et al. (2008) and Pfeifer et al. (2011) pointed out that pests could further weaken the long-term carbon storage capacity of forests by increasing the risk of forest fires, altering carbon and nitrogen cycles, and accelerating decomposition processes [6,11]. Hunt et al. (2006) highlighted that climate change might exacerbate the spread and destructive impact of invasive pests, making this issue even more complex [12]. However, significant uncertainties remain in the spatiotemporal modeling of pest outbreaks. In particular, under the complex interplay of various ecological factors—such as climate change and forest management strategies—the accuracy of predictive models requires further improvement.

Pines, belonging to the *Pinus* genus, are coniferous trees with high economic value, playing an important role in forest carbon sequestration and climate regulation [13]. Pine wood nematode (PWN) is a globally destructive invasive pest, primarily spread by the vector insect *Monochamus* beetles, which causes severe damage to highly sensitive pine species, such as Masson's pine, black pine, and oil pine [14,15]. PWD, caused by PWN, is a global forest disease [16]. It is believed that PWD originated in North America and was introduced to Asia through the inter-regional timber trade in the early 20th century [17]. In 1982, PWD was first discovered on black pine (*Pinus thunbergii* Parl) in Nanjing, Jiangsu Province, China. Since then, it has spread to surrounding counties at a rate of 7000 to

10,000 hectares per year [18]. According to the survey results from the National Forestry and Grassland Administration, PWD has occurred in 19 provinces (autonomous regions and municipalities) and 742 county-level administrative regions in China, with an affected area of 1.7165 million hectares in 2021 and 14.0792 million dead trees [19]. In recent years, PWD has spread rapidly in the Yangtze River Basin and the southeastern coastal areas of China, causing the large-scale mortality of coniferous forests [20]. This disease not only reduces the forest carbon sink function but also accelerates carbon release, further exacerbating the regional carbon balance imbalance [21]. Studies indicate that the natural recovery period of affected forests is long, with ecological functions damaged, further impacting their carbon sequestration ability [22].

The key to research on the prevention and control of pine wilt disease (PWD) lies in accurately identifying the distribution areas of the pinewood nematode (PWN) [23]. Species distribution models (SDMs), also known as ecological niche models (ENMs) or species habitat models, are tools that predict the geographic distribution of species under specific spatial and temporal conditions by correlating known species' occurrence data with relevant environmental factors using algorithms and programs [24,25]. Since the 1980s, SDMs have rapidly developed, with their theoretical framework based on the concept of ecological niches. These models are generally classified into three categories: mechanistic models, correlative models, and hybrid models [26]. Commonly used SDMs include the Bioclimatic Analysis System (BIOCLIM), the Habitat Evaluation Model (HABITAT), the Domain Environmental Model (DOMAIN), the Genetic Algorithm for Rule-set Prediction (GARP), and the Maximum Entropy Model (MaxEnt), among others. Among these, the MaxEnt model, proposed by S.J. Phillips in 2004, is particularly notable. Its core objective is to identify the maximum entropy state of the probability distribution based on known species occurrence data and environmental variable characteristics, thereby estimating the potential distribution area of a species [27–30].

The maximum entropy modeling technique is a machine learning method based on the ecological niche theory proposed by Jaynes. Initially, this method was used to estimate the density of species presence within a study area's landscape, exploring the potential suitable habitat range of target species based on species distribution data [31]. Currently, the MaxEnt model has been widely applied in species distribution predictions, accurately identifying suitable habitat areas by calculating the distribution characteristics of species-environment variable combinations under a maximum entropy state [32]. Compared with other models, the MaxEnt model exhibits significant advantages: (1) the data required for modeling are easy to obtain, no complex data preprocessing is needed, and species distribution data and environmental factor data can be directly used for modeling. (2) The model's applicability is minimally affected by temporal and spatial conditions, allowing effective simulation and prediction of suitable habitat distribution under past, present, and future scenarios. (3) Even with limited data samples, the MaxEnt model can achieve high prediction accuracy based on a small number of occurrence data points [33]. Currently, the MaxEnt model has been widely used in predicting the suitable habitat of various biological species and has played a crucial role in the prevention and control of pine wilt disease. Using this model, the potential suitable habitat distribution of the pine wood nematode can be systematically evaluated, providing scientific evidence for monitoring and controlling the disease [34,35].

Currently, several studies have used the MaxEnt model to simulate the potential distribution areas of PWN and reveal its relationship with environmental variables such as climate and topography [36,37]. However, these studies still face certain limitations: First, the existing research mainly relies on distribution point data, with monitoring data being biased in both time and space, leading to uncertainties in model predictions. Second, the

selection of environmental variables is limited and does not fully consider the impact of human activities on the spread of PWD, making it difficult to accurately simulate its diffusion mechanisms. Furthermore, most studies use default parameters without optimizing feature combinations and regularization parameters, which may lead to overfitting or underfitting of the model [38,39]. Additionally, the existing models are mostly based on static environmental variables and lack simulations of the dynamic spread of PWD under climate change scenarios. More importantly, although the threat of PWD to forest carbon stocks is increasingly severe, most studies focus on pest spread patterns and ecological impacts, with a lack of specific quantification of the carbon stock losses caused by PWN invasion. This results in an absence of systematic and accurate quantitative methods for assessing carbon stock losses, which needs to be further addressed.

The main contributions of this study are as follows:

(1) Integrates forest survey, remote sensing, and meteorological data (carbon stocks for 2002 and 2021, climate factors, and human activity data) and proposes a carbon stock loss quantification method based on the suitability distribution of pine wood nematode (PWN). This method systematically assesses the relationship between PWN suitability distribution and forest carbon stock risk, revealing the connection between disease spread and carbon stock loss.
(2) Improved model prediction accuracy and reduced the risk of overfitting through variable selection and parameter optimization. The results show that the high-suitability area for PWN expanded from 68,000 km^2 in 2002 to 184,000 km^2 in 2021 while also validating the effectiveness of the model.
(3) Quantified and assessed the dynamic risk impact of PWN on forest carbon stocks in different regions of China. The results show that the carbon risk stock increased from 87 million tC in 2002 to 99 million tC in 2021, with Guangdong Province accounting for 27.98%, showing the most significant risk.
(4) Revealed that warm, humid climates and human activities will drive the spread of PWN into the central and western regions, providing scientific evidence for disease control measures.

2. Data and Methods

2.1. Selection of Environmental Variables

The study of the spatial distribution of PWN (pine wood nematode) needs to comprehensively consider the suitable living environment for its host, the Japanese pine sawyer (*Monochamus alternatus*), the survival environment of the host tree species, and environmental variables related to the nematode itself, such as temperature, precipitation, humidity, altitude, and human activities. The influencing factors can be categorized into two types: natural variables and human variables [40]. Natural variables include climate and other environmental factors, with precipitation and temperature being core drivers of PWN occurrence and spread. From May to August, the survival and spread of pine nematodes are highly dependent on temperature and precipitation, coinciding with the peak activity and dispersal of Monochamus beetles, which are also influenced by wind speed and direction. Other natural variables include annual average temperature, precipitation, humidity, wind speed, sunshine duration, altitude, and the maximum and minimum temperatures during May to August in 2002 and 2021. Human variables are key drivers of PWN spread, with the transportation of infected dead pine trees to new areas being a critical pathway. This primarily involves assessing transportation networks (distances from outbreak counties to rivers, roads, and other transport facilities) and human activity intensity, measured using population density and land use data [41]. To ensure model accuracy, all variables have been standardized and encoded; details are provided in Table 1.

Table 1. Factors influencing the distribution of PWN in China used for modeling.

Variable Name	Variable Type	Unit	Code
Daily Average Temperature (May–August, 2002 and 2021)	Vector Data	°C	wdr
Daily Average Precipitation (May–August, 2002 and 2021)	Vector Data	mm	jsr
Daily Maximum Temperature (May–August, 2002 and 2021)	Vector Data	°C	zgwr
Daily Minimum Temperature (May–August, 2002 and 2021)	Vector Data	°C	zdwr
Daily Average Wind Speed (May–August, 2002 and 2021)	Vector Data	m/s	fsr
Daily Average Relative Humidity (May–August, 2002 and 2021)	Vector Data	%	sdr
Daily Average Sunshine Duration (May–August, 2002 and 2021)	Vector Data	h	rzr
Annual Average Precipitation (2002 and 2021)	Vector Data	mm	jsn
Annual Average Temperature (2002 and 2021)	Vector Data	°C	qwn
Annual Average Wind Speed (2002 and 2021)	Vector Data	m/s	fsn
Annual Sunshine Duration (2002 and 2021)	Vector Data	h	rzn
Annual Average Relative Humidity (2002 and 2021)	Vector Data	%	sdn
Total Population Data (2002 and 2021)	Raster Data	Person	hfp
Land Use Data (2002 and 2021)	Raster Data	km^2	clcd
PWD-Affected Counties (2002 and 2021)	Raster Data	a	bf
Distance from PWD Outbreak Points to Railways (2002 and 2021)	Raster Data	km	tlos
Distance from PWD Outbreak Points to Roads (National Highways, Expressways, Urban Expressways, Provincial Roads, and Other Major Roads, 2002 and 2021)	Raster Data	km	glos
Distance from PWD Outbreak Points to China's Primary Rivers (2002 and 2021)	Raster Data	km	yjh
Distance from PWD Outbreak Points to China's Secondary Rivers (2002 and 2021)	Raster Data	km	erjih
Distance from PWD Outbreak Points to China's Tertiary Rivers (2002 and 2021)	Raster Data	km	sjh
Digital Elevation Model (DEM, 30-m resolution)	Raster Data	m	alt
Slope Aspect Extracted from DEM (30-m resolution)	Raster Data	°	asp
Slope Gradient Extracted from DEM (30-m resolution)	Raster Data	°	slo

2.2. Data Sources

This study selected 23 natural ecological factors, including climate, topography, distance to water systems, distance to roads, and human activities, for constructing the MaxEnt model. All factors were standardized to 30″-resolution ASCII raster files. Climate data were obtained from NOAA's NCEI (https://www.ncei.noaa.gov/data/global-summary-of-the-day/archive/ (accessed on 6 February 2025)) [42]. The land use data are sourced from the team of Yang Jie and Huang Xin at Wuhan University (https://zenodo.org/records/12779975 (accessed on 6 February 2025)). Data on human-intervened land use types and water system features were extracted using a raster calculator [40]. Population density data were obtained from SEDAC (https://sedac.ciesin.columbia.edu/ (accessed on 6 February 2025)) [43], and road density data came from the GRIP Global Roads Database (https://www.globio.info/ (accessed on 6 February 2025)) [44]. To model the cost layer, human disturbance factors were standardized and weighted using the entropy weighting method in R [45]. Data on PWD-affected counties in China were obtained from the National Forestry and Grassland Administration's Biological Disaster Prevention and Control Center (http://www.forestry.gov.cn/main/6206/20220406/151041215456755.html (accessed on 6 February 2025)), which compiles biannual reports from county forestry bureaus. This study also utilized the "Vegetation Atlas of China" (1:1,000,000) and the CASEarth vegetation distribution dataset (https://www.plantplus.cn/dsite/zhibei/b12.html, https://www.bio-one.org.cn) [46,47] to map forest tree species distributions. Forest

carbon stock data from 2002 to 2021 were sourced from the "National Tibetan Plateau Data Center" (http://data.tpdc.ac.cn) [48]. The map mentioned in the text is based on the world map downloaded from the Standard Map Service System of the Map Technology Review Center of the Ministry of Natural Resources of the People's Republic of China, with the review number GS(2020)4619. The base map has not been modified.

2.3. Main Environmental Variable Screening

This study utilized an optimized MaxEnt model to analyze the potential habitat suitability of pine wood nematodes in China for 2002 and 2021. The jackknife method was applied to assess the contribution and importance of environmental factors to PWN distribution, while response curves were used to predict the range of suitable habitats and identify how key factors constrain distribution. To reduce the effects of high correlation and collinearity among environmental factors, the initial model employed MaxEnt's jackknife method to exclude variables with low predictive contributions. For variables with high contributions, Spearman correlation analysis was conducted to minimize autocorrelation and enhance model accuracy [49]. The MaxEnt analysis was performed using MaxEnt 3.44 software (developed by Steven J. Phillips' team at Columbia University, New York, NY, USA), and Spearman correlation analysis was conducted in R.

2.4. Construction of the MaxEnt Model

The principle of maximum entropy is a mathematical method used to infer unknown information from limited known information. Its core principle is to preserve all uncertainties, meaning that, in the absence of subjective assumptions, the probability distribution with the maximum entropy value minimizes risk [50]. Assuming the probability distribution of a discrete random variable x is P(x), the entropy is calculated using the following formula:

$$\mathrm{H}(P) = \sum_x P(x) log P(x) \quad (1)$$

When x follows a uniform distribution, the entropy reaches its maximum. Additionally, the entropy satisfies the following inequality:

$$0 \leq \mathrm{H}(P) \leq \log|x| \quad (2)$$

This study conducted simulations using MaxEnt 3.4.4. The formula for the MaxEnt model is as follows:

$$P_w(y/x) = \frac{1}{Z_w(x)} exp\left[\sum_{i=1}^{n} w_i f_i(x,y)\right] \quad (3)$$

$$Z_w(x) = \sum_{i=1}^{n} exp\left[\sum_{i=1}^{n} w_i f_i(x,y)\right] \quad (4)$$

In Equations (3) and (4), x represents the input environmental variables, y denotes the geographical locations of pine wood nematode (PWN) occurrence, $f_i(x,y)$ is the feature function, w_i is the weight of the feature function, n is the number of data points in the dataset, $Z_w(x)$ is the weight function of the environmental variables, and $P_w(y/x)$ represents the suitability of PWN. The model was run using a subsampling method, where 70% of the sample points were randomly selected as the training dataset, and the remaining 30% were used as the testing dataset. The convergence threshold was set to 10^5, and training stopped when the log loss of each iteration fell below the threshold. The output format selected for predicting the distribution was "Logistic", which outputs values between 0 and 1. These values represent probabilities and can be interpreted as relative suitability [51].

2.5. Classification of Potential Suitable Habitat Levels for Pine Wood Nematode in China

Using the optimized model, ArcGIS 10.8 was employed to reclassify simulation results and generate potential distribution maps, with non-suitable and suitable areas defined using the Maximum Training Sensitivity Plus Specificity (MTSS) threshold [52]. The results were based on species presence probability values (P) and generated as ASCII raster layers, with P values ranging from 0 to 1, where higher P values indicate higher species presence probability. The MTSS threshold in this study was set to 0.173, classifying areas as non-suitable (0–0.173), low suitability (0.173–0.4), medium suitability (0.4–0.6), high suitability (0.6–0.8), and optimal suitability (0.8–1). To quantify current and future habitat changes for pine wood nematodes, the area of each suitability category was calculated based on the MTSS threshold, with habitat suitability levels defined as high (0.6–1), medium (0.4–0.6), low (0.2–0.4), and non-suitable (0–0.2) [18].

2.6. High-Risk Forest Carbon Stocks

To assess the potential loss of carbon stocks in China's forest ecosystems caused by the invasion of PWN, which is critical for carbon sequestration risk evaluation, we derived the calculation equation for carbon stocks in forests affected by PWN risk (*CFPWDR*) as follows:

$$CFPWDR = HSA \times (AGBC + BGBC) \quad (5)$$

HSA represents the area of high-sensitivity host tree species for PWN within the suitable habitat predicted by the MaxEnt model in China. *AGBC*, measured in tons of carbon per hectare (tC/ha), indicates the carbon stock stored aboveground in forest trees. Similarly, *BGBC*, also measured in tC/ha, reflects the carbon stock stored in root systems. The integration of these indices provides a comprehensive measure of the vulnerability of forest carbon stocks to loss. The application of this formula illustrates the potential impact of PWN invasion on aboveground and belowground carbon stocks in China's forests, quantifying the risks to forest carbon sequestration capacity.

3. Results and Analysis

3.1. Overall Trends of PWD

From Figures 1 and 2, it is evident that, since the outbreak of PWD in China in 1982, the disease has shown a trend of "increase-decrease-increase" across 20 provinces, with an explosive growth phase in 2018. The number of affected counties rose from 3 in 1982 to a peak of 615 in 2021, slightly decreasing to 586 in 2022. Between 1982 and 2000, the disease spread from Nanjing, Jiangsu, to the Yangtze River Basin and southeastern coastal regions (Zhejiang, Jiangsu, Anhui), with limited expansion. From 2000 to 2013, the spread accelerated, with Zhejiang becoming a heavily affected area and Guangdong, Fujian, and other southern coastal provinces seeing increased impact. The 2013–2018 period marked an explosive growth phase, with affected counties rising from 206 to 500, spreading to Henan, Hunan, Hubei, and southwestern regions. From 2018 to 2022, the number of affected counties remained high, with the Yangtze River Basin and eastern coastal regions being the most severely impacted. Zhejiang and Jiangsu reported 65–70 affected counties, while Guangdong, Guangxi, and Sichuan continued to expand. Overall, PWD has shown a regional high-incidence and sustained spread trend, with potential future expansion driven by climate and forest ecosystem changes. Strengthened monitoring and control measures are urgently needed to mitigate its long-term threat.

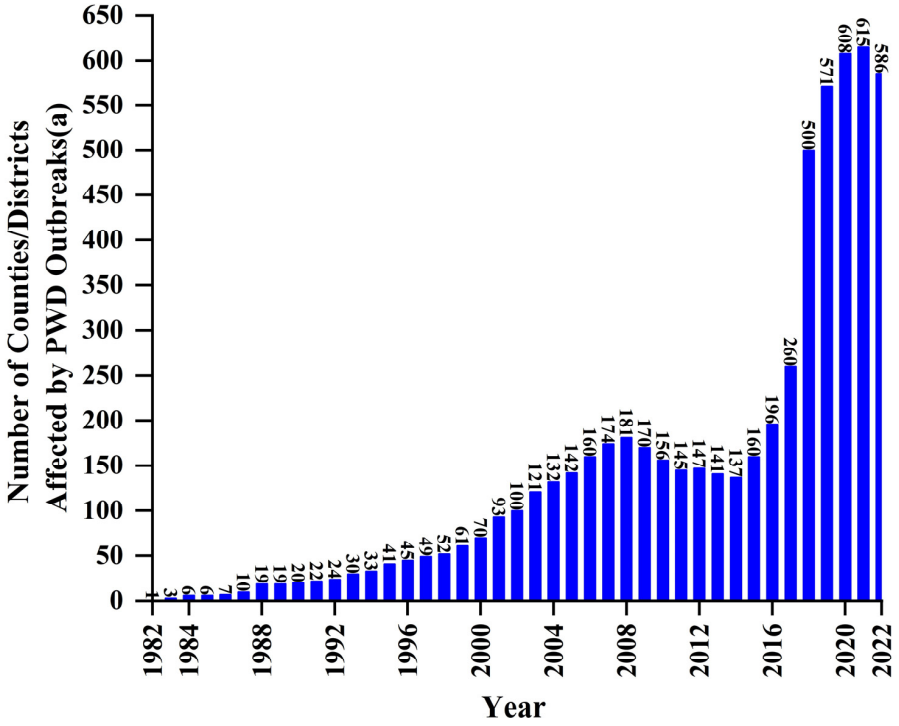


Figure 1. Number of counties and districts affected by PWD in China from 1982 to 2022.

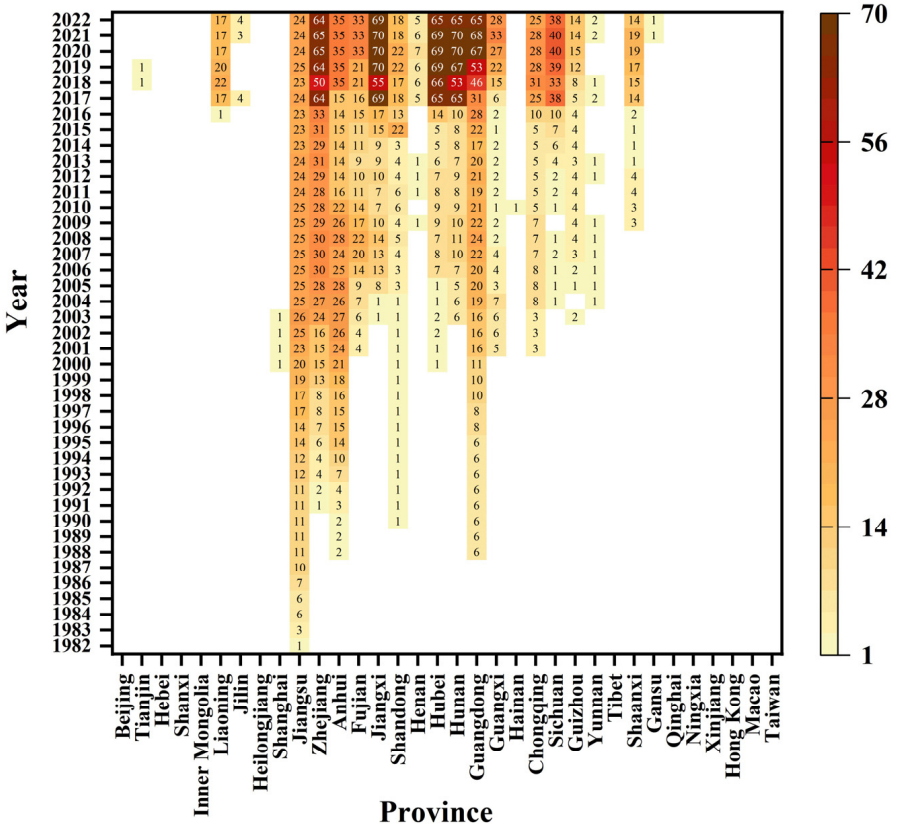


Figure 2. Statistics on the number of affected counties in provinces, municipalities, and autonomous regions in China over the past 40 years.

3.2. Spatial Distribution Analysis of Resistance Levels of Host Tree Species to Pine Wood Nematode in China

Different pine species exhibit significant variations in susceptibility to PWN, making it essential to categorize host species and their resistance indices to assess carbon loss risks

caused by pest infestations. Using the "Vegetation Atlas of China" (1:1,000,000) and the "1:500,000 China Vegetation Distribution Dataset", this study extracted data on coniferous and mixed forests for 2002 and 2021, classifying pine species into highly susceptible and low-susceptible groups (see Table 2). Figure 3 shows that highly susceptible species are concentrated in the southeastern hills and coastal humid regions, while low-susceptible species are found in southwestern high-altitude and northern cold regions, highlighting adaptive differences. Environmental factor analysis reveals that, in 2002, the primary factors were population density (hfp, 31.7%) and altitude (alt, 27.7%), whereas in 2021, mean annual humidity (sdn, 49.8%) was the dominant factor, with human activity having a significantly increased impact (Table 3).

Table 2. Sensitivity classification of host tree species to PWN.

Pine Tree Species	PWN Resistance Sensitivity
Japanese red pine, black pine, Korean red pine, Chinese red pine, Mason's pine, Yunnan pine	Highly sensitive
Alpine pine, Hainan Province, Chinese white pine, needle pine, Ludjun pine, Simao pine, Bashan pine, Chinese white-barked pine, larch, torch pine, Xingkai pine, creeping pine, Siberian pine, etc.	Low sensitivity

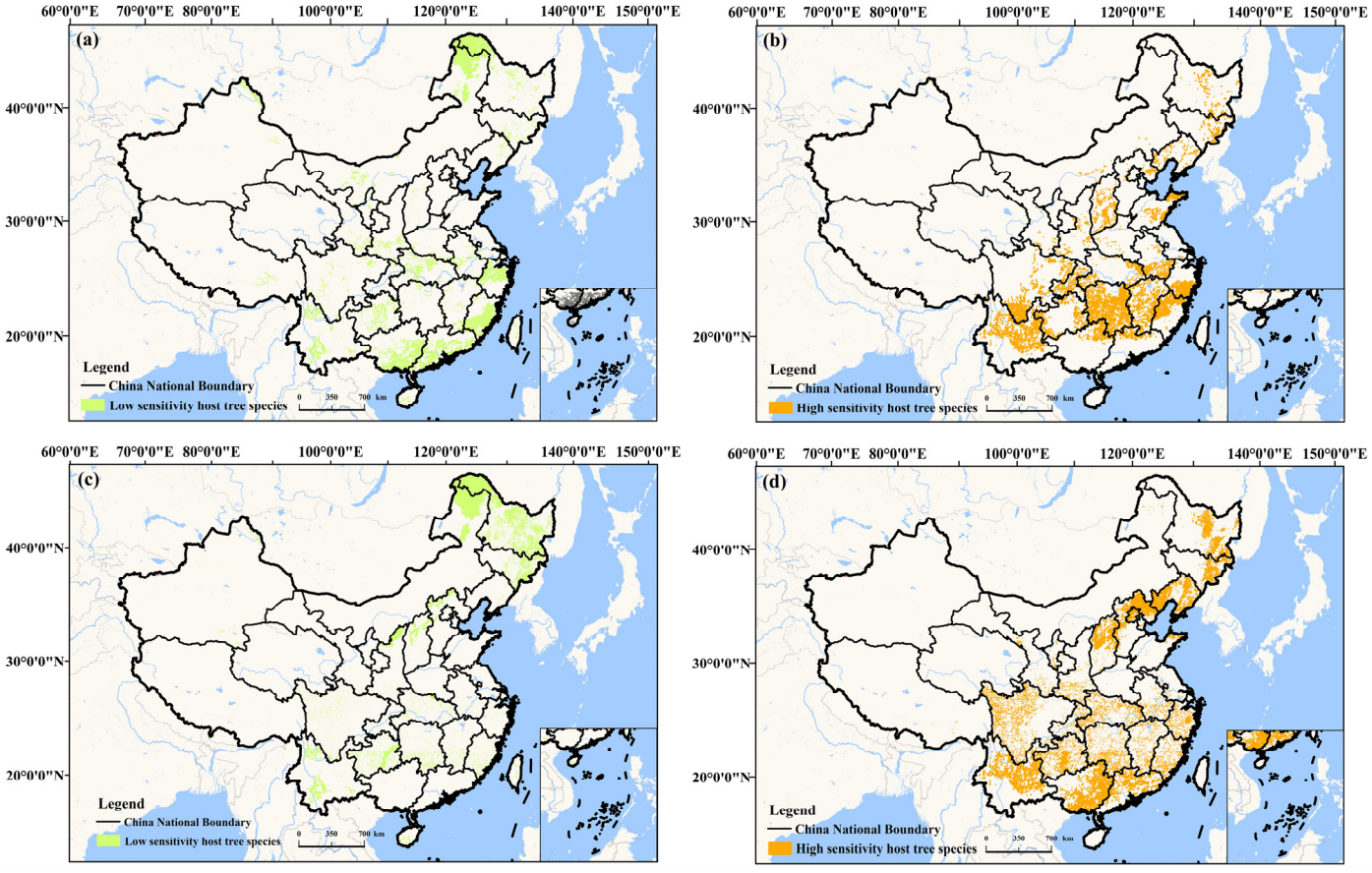


Figure 3. Spatial distribution of resistance levels of PWN host tree species. The orange areas in the figure represent regions where high-sensitivity PWN host tree species grow, while the green areas represent regions of low-sensitivity PWN host tree species. The sensitivity level classifications are as follows: (**a**) the distribution of high-sensitivity host tree species in 2002; (**b**) the distribution of low-sensitivity host tree species in 2002; (**c**) the distribution of high-sensitivity host tree species in 2021; and (**d**) the distribution of low-sensitivity host tree species in 2021.

Table 3. Contribution rates and importance of different environmental factors to the MaxEnt model for PWN.

Environmental Variables (2002)	Contribution Rate (%)	Importance (%)	Environmental Variables (2021)	Contribution Rate (%)	Importance (%)
hfp	31.7	0.4	sdn	49.8	6.8
alt	27.7	57	alt	11.4	23.3
qwm	17.7	0.1	hfp	10.4	2
yjh	9.9	8.1	jsr	7.6	2.7
rzn	3.7	6.8	rzn	6.6	1.1
sdr	3.2	8	qwn	6.3	22.9
sdn	1.5	3.6	wdr	2.3	4
glos	1.3	10.3	tlos	1.6	7
fsr	1.2	1.1	fsr	1.3	7.3
slo	1.1	2.9	glos	0.8	9.5
zgwr	0.3	0	sjh	0.8	6.6
zdwr	0.3	1.1	yjh	0.6	2
asp	0.2	0	clcd	0.3	0.6
sjh	0.1	0.2	fsn	0.3	3.9
jsn	0.1	0	zgwr	0.1	0.2
clcd	0	0			
tlos	0	0.4			
fsn	0	0			

3.3. Analysis of Suitable Habitat Areas for Pine Wood Nematode in China

3.3.1. Key Environmental Factors Influencing the Distribution of Pine Wood Nematode

Figure 4a shows that most factor pairs have strong correlations, with many factors having correlation coefficients close to 1 or −1, indicating significant positive correlations (red) and negative correlations (green). In particular, the daily maximum temperature in May–August 2002 (zgwr) and the daily minimum temperature in May–August 2002 (zdwr) show near-perfect positive correlation (correlation coefficient close to 1). In Figure 4b, the correlation distribution changes, with significantly more factor pairs having weak correlations (yellow areas), indicating increased independence between factors and a reduction in the proportion of strong positive and negative correlations. Additionally, in Figure 4a, the correlation coefficient between the daily maximum temperature in May–August 2002 (zgwr) and the daily minimum temperature in May–August 2002 (zdwr) is 1, showing a perfect positive correlation. The correlation between the average daily sunlight in 2002 (rzn) and the average daily sunlight in May–August 2002 (rzr) is also high (around 0.95–1.0), suggesting that these factors may interact synergistically in the same environmental mechanism to affect PWN. The negative correlation between altitude (alt) and aspect (asp) is relatively strong (correlation coefficient around −0.6 to −0.7), implying that they may have mutually restrictive or opposing ecological functions. In Figure 4b, the factor pairs with strong positive correlations (such as the average daily sunlight in 2021 (rzn) and the average daily sunlight in May–August 2021 (rzr), with a correlation coefficient still around 1) are still prominent, but negative correlations have decreased. Figure 5 indicates that suitable habitats in 2002 were concentrated in low-altitude, warm climates, and areas near rivers, while in 2021, suitability peaked at rainfall levels of 10–12 mm and expanded further under

the influence of human activities. Overall, altitude remains a key limiting factor, and future control efforts should focus on low-altitude and densely populated areas.

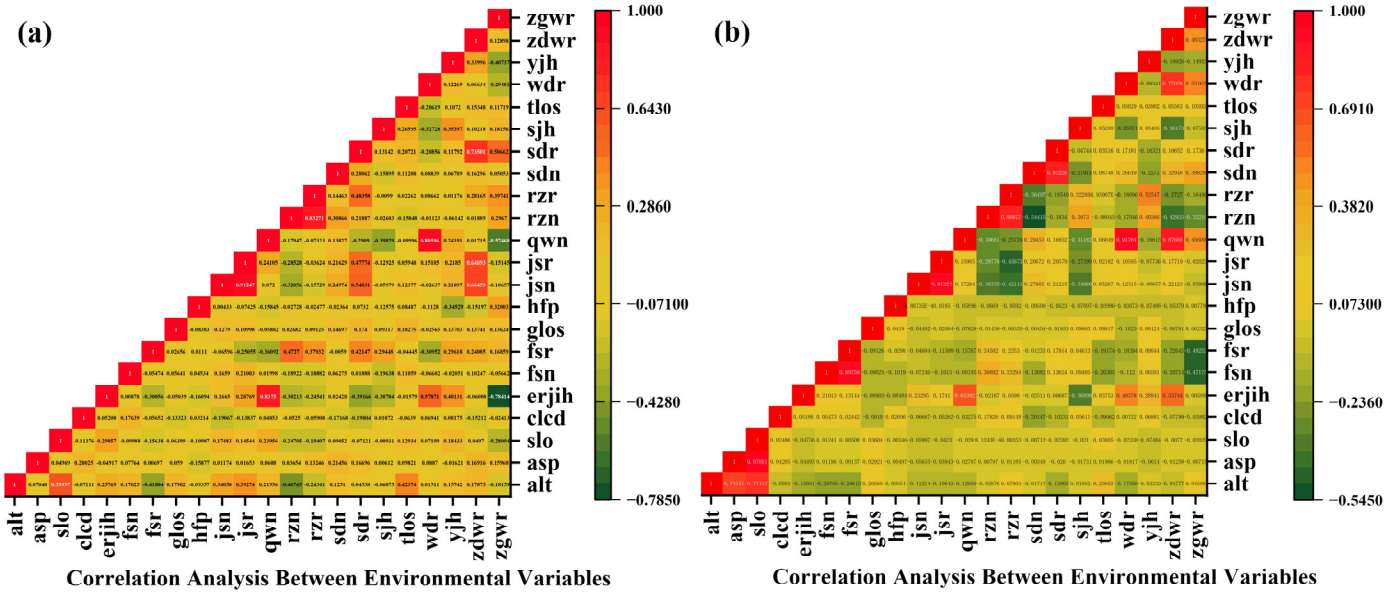


Figure 4. Distribution of correlation coefficients between environmental factors for PWN: (**a**) distribution of correlation coefficients between environmental factors for PWN in 2002; (**b**) distribution of correlation coefficients between environmental factors for PWN in 2021.

Changes in the time dimension: The correlation coefficient range in Figure 4a is from −0.785 to 1.000, while in Figure 4b, the range narrows to −0.545 to 1.000, indicating an increase in the proportion of weaker correlations. By comparing the two figures, it can be seen that the negative correlation between alt and asp has significantly weakened (from about −0.7 to −0.4), while the strong positive correlation between the average daily sunlight in 2002 (rzn) and the average daily sunlight in May–August 2002 (rzr) remains unchanged.

In Figure 4a, factor pairs with absolute correlation coefficients greater than 0.5 account for over 60% of the total, showing a strong correlation between factors. In Figure 4b, the factor pairs with absolute correlation coefficients greater than 0.5 decrease to about 30%–40%, indicating a general weakening of the correlations between factors and an increase in independence. This suggests that the relationships between some factors have significantly changed between the two stages, possibly due to the influence of climate, environmental, or human factors.

3.3.2. Optimization and Accuracy Evaluation of the MaxEnt Model

Key parameters for optimizing the MaxEnt model include feature combinations (FCs) and the regularization multiplier (RM). With the R package ENMeval, the optimal parameters were selected based on AICc values. Both 2002 and 2021 models adopted linear (L) and quadratic (Q) feature combinations (LQ), with RM optimized at 1.0 to avoid overfitting (Figure 6). Model performance was evaluated using AUC values, with 2002 achieving an AUC of 0.975 (“very good”) and 2021 an AUC of 0.907 (“good”), demonstrating high model stability (Figure 7). Jackknife analysis revealed that, in 2002, PWN distribution was primarily influenced by natural factors, with altitude (alt, gain 1.4) and slope (asp, gain 1.0) being the most significant contributors, resulting in a total training gain of 2.6. By 2021, human activities, such as land use (clcd, gain 0.8) and population density (hfp, gain 0.7), played a greater role, reducing the total gain to 1.3 (Figure 8). A comparison shows that natural factors dominated in 2002, while human influence increased significantly by 2021, weakening the role of natural constraints. Figure 5 indicates that suitable habitats were

concentrated in low-altitude areas, with 2021 suitability more strongly correlated with moderate precipitation (10–12 mm) and densely populated regions. Future strategies should integrate natural factors (altitude, temperature, and precipitation) and human factors (land use and population density) to improve predictions of PWN spread and inform effective control measures.

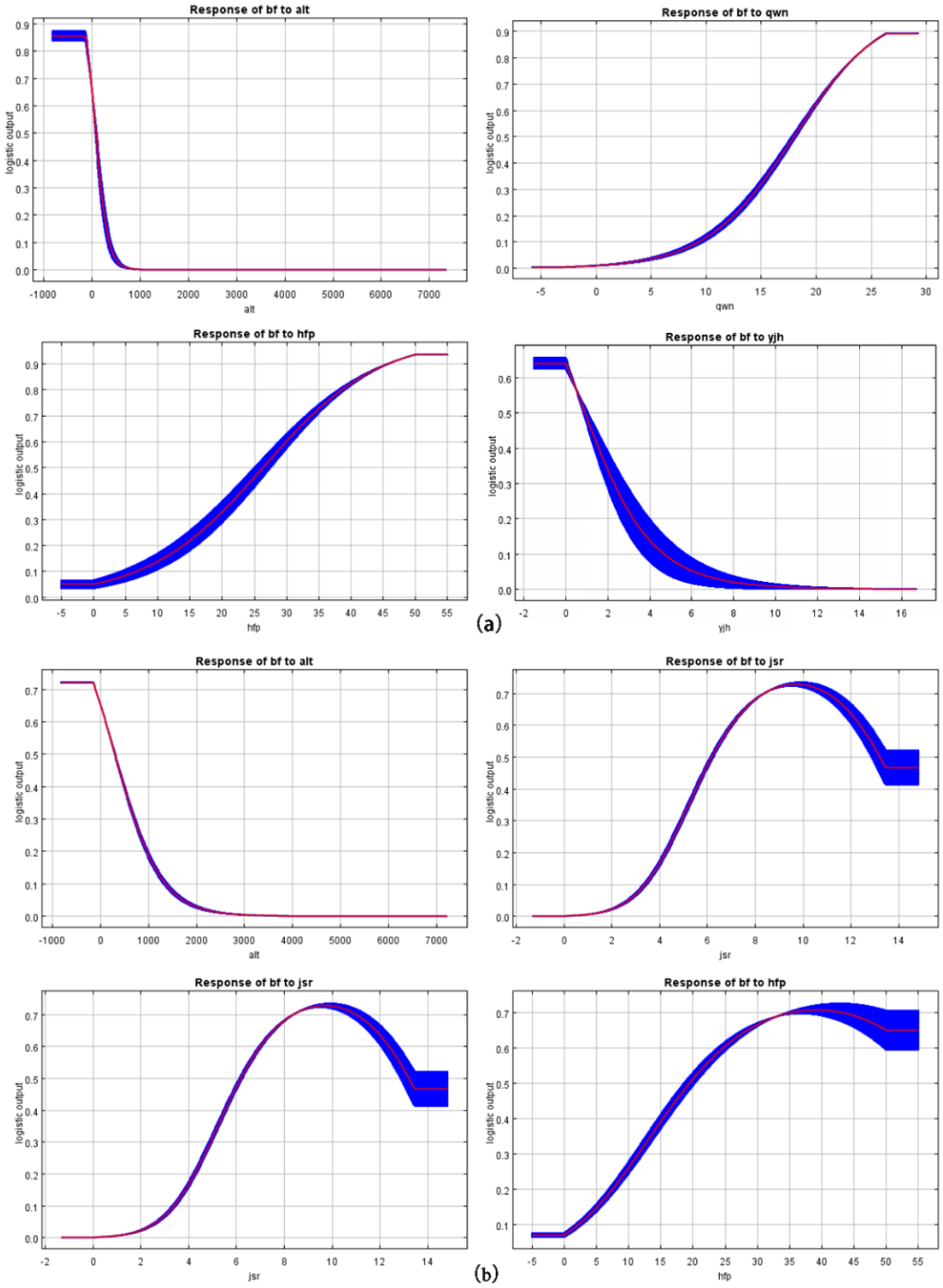


Figure 5. Response curves of key environmental factors. (**a**) Response curves of key habitat factors in the prediction of PWN suitable areas in 2002 based on the model; (**b**) response curves of key habitat factors in the prediction of PWN suitable areas in 2021 based on the model. Note: Blue lines represent the model's predicted output, and red is used to show the actual observed results or baseline values. The comparison between the two is used to evaluate the model's prediction accuracy.

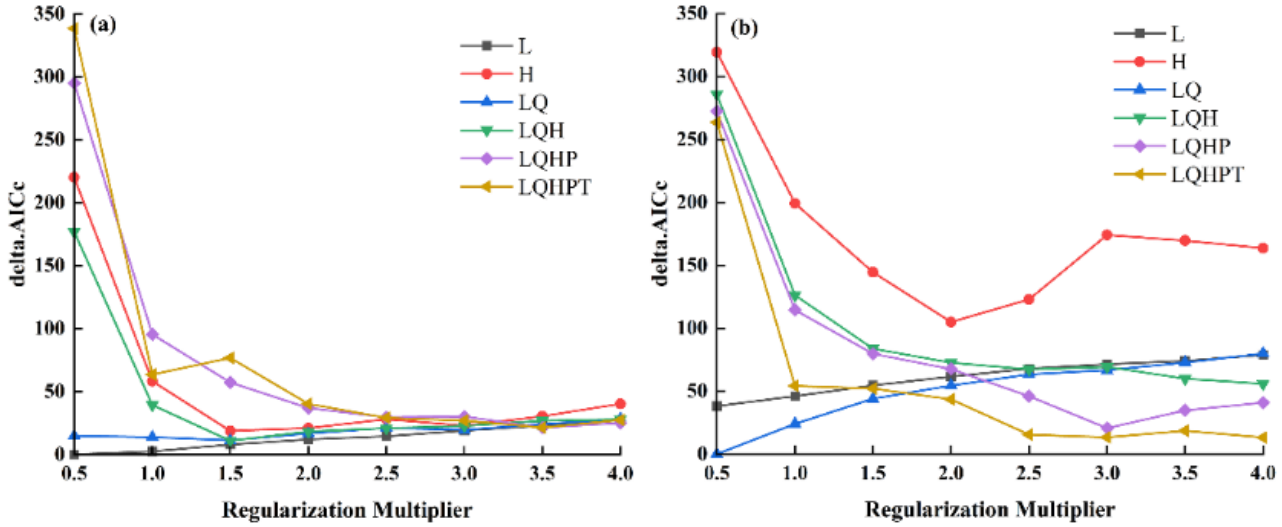


Figure 6. Optimization results of the MaxEnt model using ENMeval. (**a**) The optimization results of the MaxEnt model in 2002; (**b**) The optimization results of the MaxEnt model in 2021.

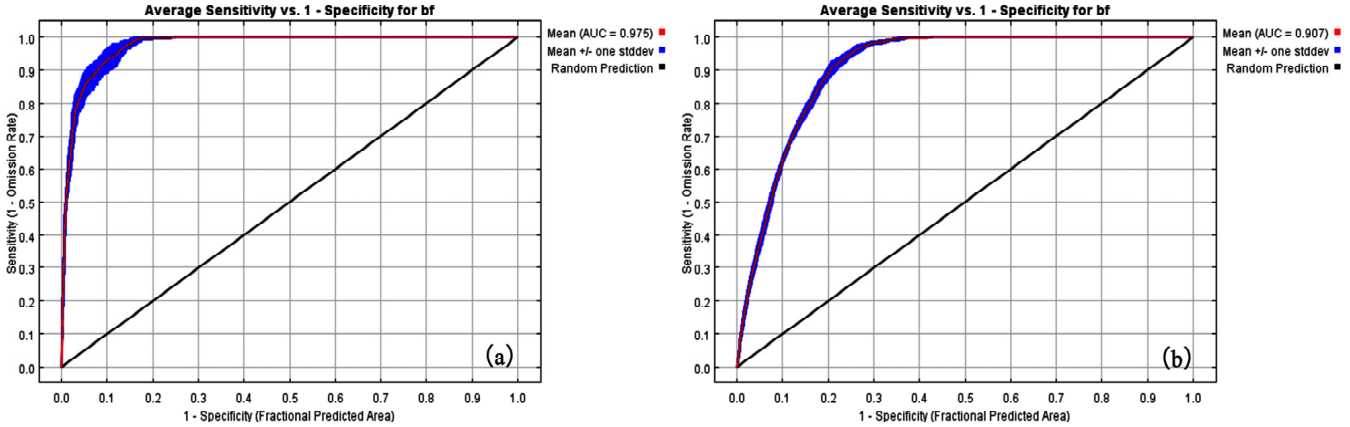


Figure 7. AUC curves of the habitat suitability model for PWN in China. (**a**) MaxEnt model based on environmental factors in 2002; (**b**) MaxEnt model based on environmental factors in 2021.

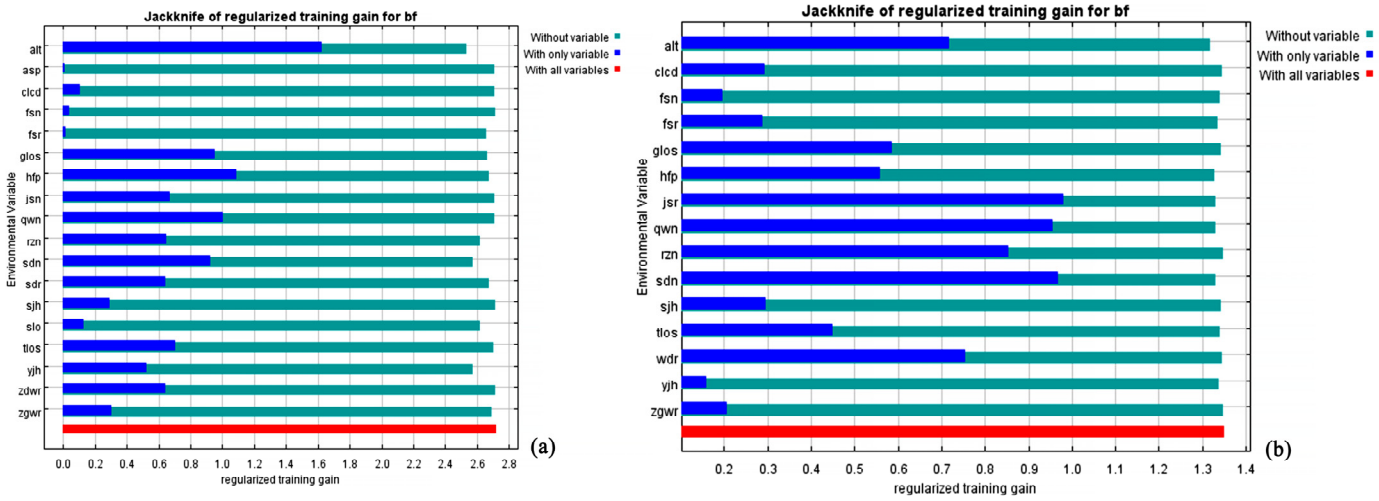


Figure 8. Jackknife test results. (**a**) Jackknife test results for the 2002 simulation; (**b**) Jackknife test results for the 2021 simulation.

3.3.3. Analysis of Potential Suitable Habitat Simulation for Pine Wood Nematodes

According to Figures 9 and 10, the suitability areas for PWN in China underwent significant changes from 2002 to 2021. Low-suitability areas decreased, medium-suitability areas expanded, and high-suitability areas increased substantially. The area of low-suitability regions shrank from 989,000 km^2 in 2002 to 415,000 km^2 in 2021, a reduction of 574,000 km^2. For instance, Guangdong decreased from 42,000 km^2 to 4400 km^2, and Chongqing from 101,000 km^2 to 32,100 km^2, while Inner Mongolia, Ningxia, and Xinjiang showed minimal changes. Medium-suitability areas increased from 104,000 km^2 to 362,000 km^2, an expansion of 258,000 km^2, with Sichuan growing from 1300 km^2 to 83,800 km^2 and Henan from 3900 km^2 to 18,900 km^2, indicating that climate change has gradually made conditions favorable for PWN spread in central and western regions. High-suitability areas expanded significantly, from 68,000 km^2 to 184,000 km^2, an increase of 116,000 km^2. This growth was particularly notable in eastern coastal areas, with Zhejiang expanding from 12,600 km^2 to 47,000 km^2 and Shanghai from 1600 km^2 to 4400 km^2. Conversely, high-suitability areas in Hunan and Guangdong decreased significantly due to improved control technologies, with Guangdong reducing from 101,700 km^2 to 37,500 km^2 and Hunan from 107,500 km^2 to 36,000 km^2. Overall, suitability areas in the eastern coastal and central-western regions have grown markedly. Future efforts should focus on high-risk areas and the gradually suitable central–western regions, strengthening monitoring and control to protect forest ecological security.

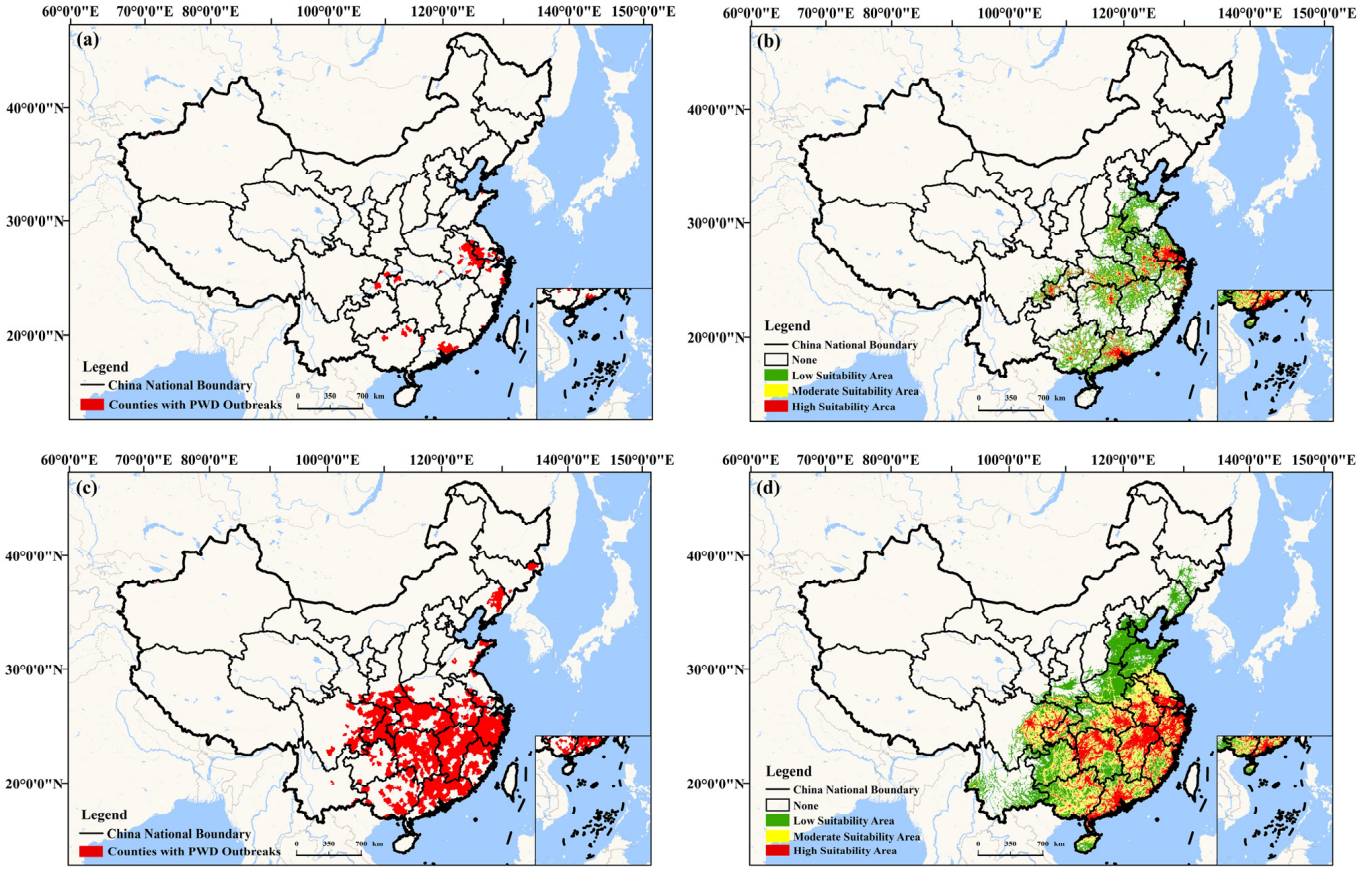


Figure 9. Distribution of suitable areas for PWN under the influence of different climatic variables. (**a**) Counties affected by PWD in 2002; (**b**) spatial distribution of suitable areas for PWN in 2002; (**c**) counties affected by PWD in 2021; (**d**) spatial distribution of suitable areas for PWN in 2021. Note: the suitable areas for the pine wood nematode (PWN) identified in this study represent potential distribution regions and do not imply that these areas have already experienced PWD outbreaks.

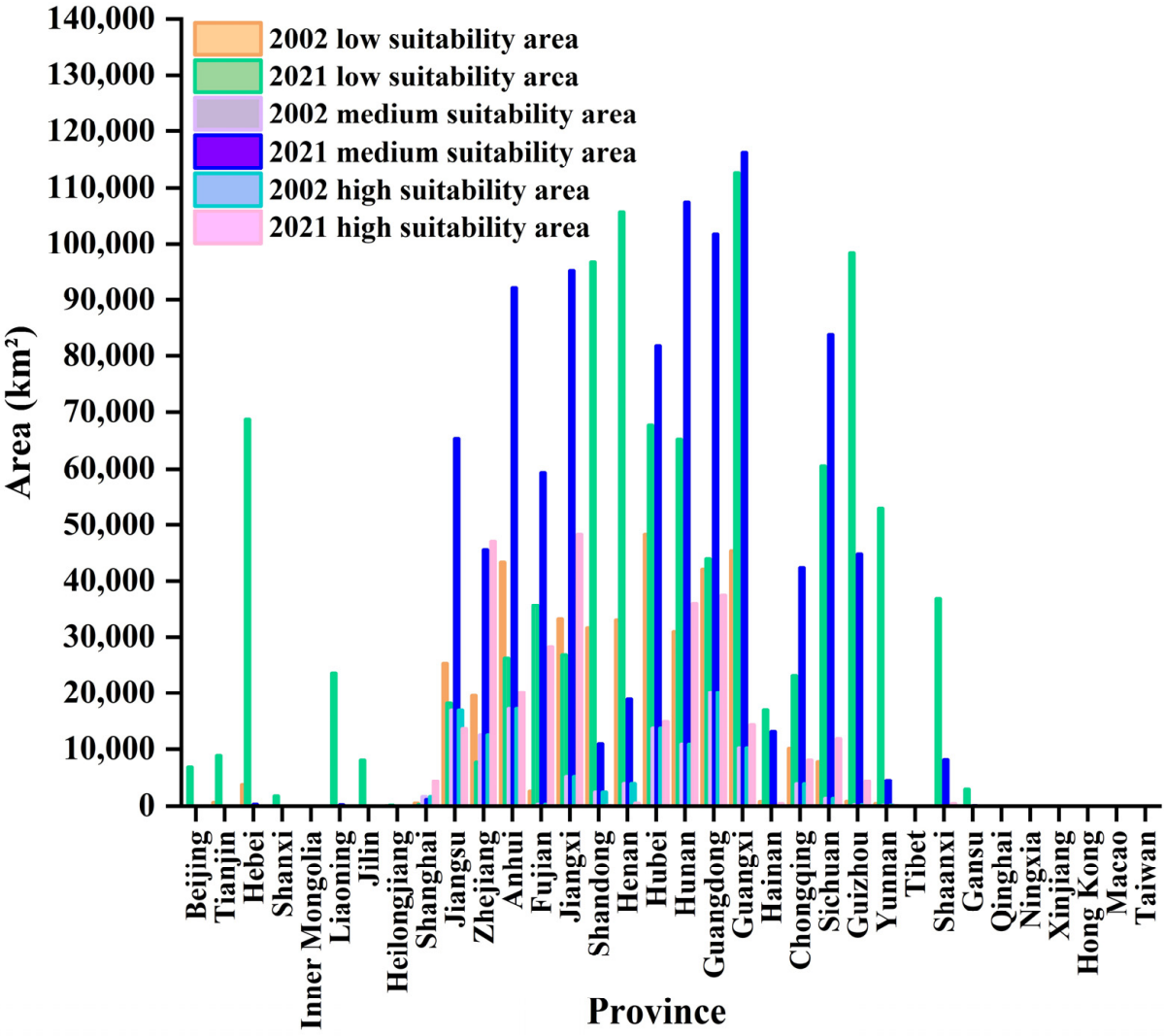


Figure 10. Potential suitable areas for PWN in China in 2002 and 2021.

3.4. Spatial Distribution of Host Tree Sensitivity Levels and Carbon Stock Analysis

3.4.1. Analysis of Aboveground and Belowground Carbon Stocks in China's Forests

Figure 11 shows significant growth in China's aboveground and belowground forest carbon stocks from 2002 to 2021, with a broader distribution. In 2002, the aboveground carbon stock was 84.1 billion tons, and the belowground carbon stock was 30.7 billion tons, accounting for 25%–30% of the total, mainly concentrated in southwestern (Yunnan, Sichuan, and Guizhou) and northeastern (Heilongjiang, Jilin, and Inner Mongolia) regions (Figure 11a,b). By 2021, aboveground carbon stock had increased to 126.1 billion tons, and belowground carbon stock to 43.2 billion tons, representing growth of 50% and 41%, respectively. High-value areas expanded to southeastern coastal regions (Fujian, Guangdong, and Guangxi), reflecting the effectiveness of ecological protection and afforestation projects (Figure 11d,e). Figure 11c,f indicate that in 2021, Yunnan's aboveground carbon stock reached 1.75 billion tons (21% increase), and belowground carbon stock reached 378 million tons (22% increase). Heilongjiang recorded 1.445 billion tons of aboveground carbon (12% increase) and 468 million tons belowground. Sichuan had 1.307 billion tons of aboveground carbon (21% increase) and 287 million tons belowground, while Inner Mongolia's stocks were 953 million tons aboveground and 367 million tons belowground, making them key high-carbon-stock regions. Low-carbon-stock regions (e.g., Beijing, Tianjin, and Shanghai) showed significant growth, with Tianjin's aboveground carbon stock increasing

from 660,000 tons to 1.5 million tons (127% increase). Overall, China's forest ecological restoration and carbon storage capacity have improved, with high-carbon-stock provinces (Yunnan, Heilongjiang, Sichuan, and Inner Mongolia) standing out and achieving a more balanced distribution.

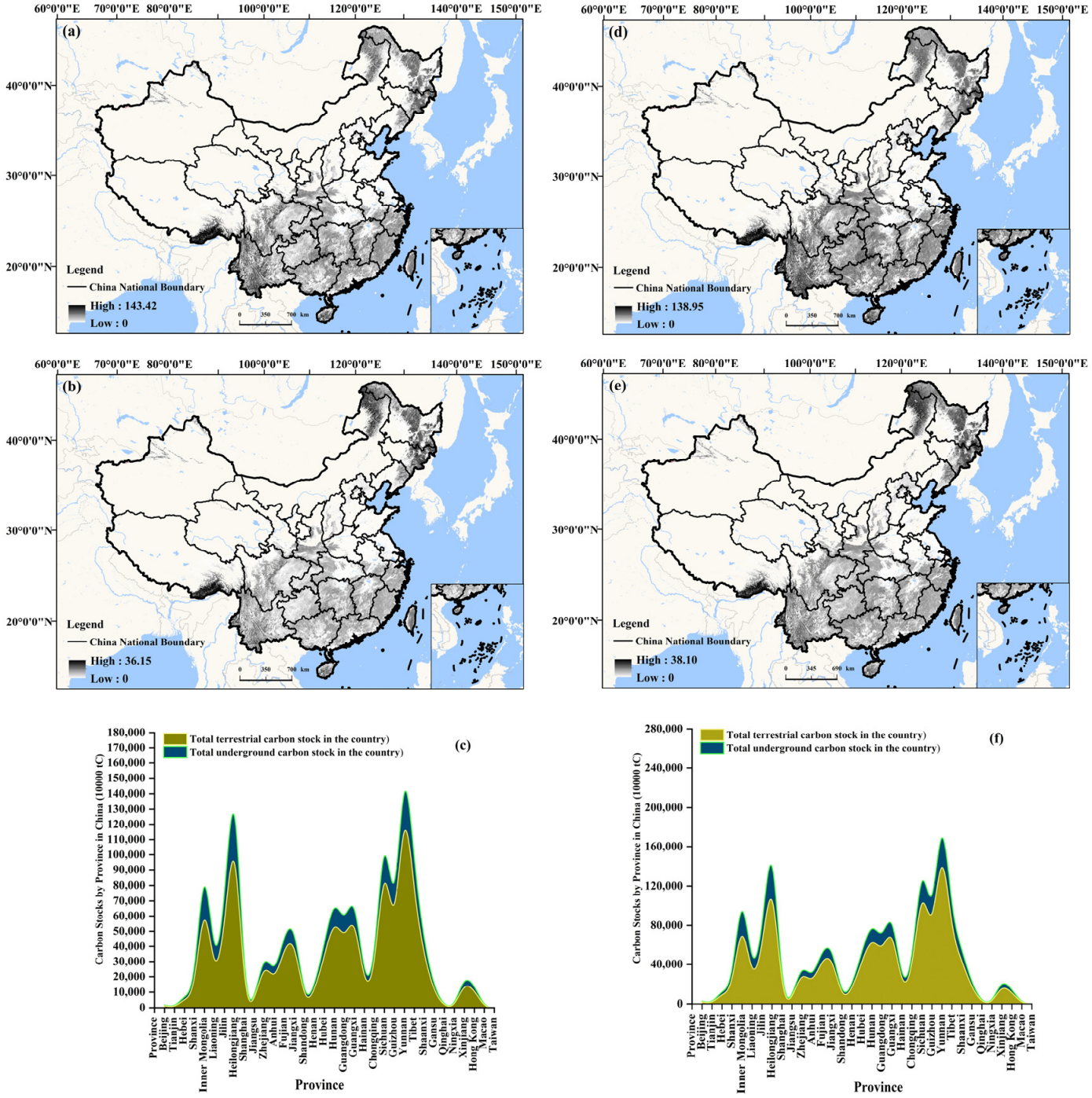


Figure 11. Aboveground and belowground carbon stocks (t/C) of PWN host tree species in China. (**a**) Distribution of aboveground forest carbon stocks in China, 2002; (**b**) distribution of belowground forest carbon stocks in China, 2002; (**c**) green and blue bars represent the carbon content of aboveground and belowground components in 2002, respectively (10,000 t/C); (**d**) distribution of aboveground forest carbon stocks in China, 2021; (**e**) distribution of belowground forest carbon stocks in China, 2021; (**f**) green and blue bars represent the carbon content of aboveground and belowground components in 2021, respectively (10,000 t/C).

3.4.2. Provincial Classification and Key Regional Analysis of Risk Carbon Stocks in PWN Host Tree Species in China

Figure 12 shows that, from 2002 to 2021, China's total aboveground and belowground forest carbon stocks increased significantly, rising from 11.134 billion tC to 16.805 billion tC, an increase of approximately 5.671 billion tC (over 50%). This growth is mainly attributed to the implementation of afforestation, reforestation, and ecological conservation policies, with particularly notable increases in the southwestern regions, such as Yunnan and Sichuan. However, the carbon stocks affected by pinewood nematode (PWN) also increased during the same period, rising from 0.087 billion tC in 2002 to 0.099 billion tC in 2021. In 2002 (Figure 12a), high-risk carbon stock areas were concentrated in the southwest (e.g., Sichuan, Tibet, Yunnan) and the northeast (e.g., Heilongjiang, Inner Mongolia). By 2021 (Figure 12c), the southwestern region had further solidified its status as a core area of carbon stock growth. Meanwhile, PWN-affected carbon stocks expanded from the eastern and central regions (e.g., Anhui, Hunan, and Zhejiang) to the southern and southwestern regions (e.g., Guangdong and Guizhou) (Figure 12b,d). Guangdong Province's risk proportion rose from less than 1% in 2002 to 27.98% in 2021, with its risk carbon stock increasing from 0.03 billion tC to 0.17 billion tC, making it the highest-risk province in the country. Guizhou's risk proportion also increased to 6.11%. In contrast, Anhui and Hunan, which had the highest risks in 2002 (6.08% and 4.72%, respectively), saw their proportions drop to 1.07% and 1.00% by 2021, indicating a shift in risk distribution (Figure 12e,f). Overall, the spread of PWN has shifted from the traditional eastern regions to the southern and southwestern regions, driven primarily by the warm and humid climate in the south. In contrast, the northern and northwestern regions (e.g., Heilongjiang and Inner Mongolia) exhibit relatively low risks, with more stable forest ecosystems. Moving forward, priority should be given to monitoring high-risk PWN areas in southern and southwestern China to mitigate the threat of PWN to forest ecosystems.

Figure 13 shows that, in 2021, the forest carbon storage risk areas in China were mainly concentrated in Guangdong, Guangxi, Guizhou, Zhejiang, Yunnan, Liaoning, Hubei, and Tianjin. These regions have the highest carbon risk amounts and percentages, reflecting a significant threat to China's forest carbon storage in these risk areas.

Figure 13a (left map) shows the amount of forest carbon storage in each province under the risk of PWN (pine wood nematode disease), with different shades of color representing the magnitude of forest carbon storage in each province, in units of 10,000 tons of carbon (tC). Guangdong has the highest forest carbon storage, with 17.5 million tons of carbon, accounting for 27.98% of the national total. Other provinces such as Guangxi, Guizhou, and Zhejiang also have high forest carbon storage, particularly in Guangdong, Guangxi, and Guizhou, where the forest carbon storage in the PWN risk areas plays an important role and may face significant carbon storage loss. Figure 13b (right map) shows the percentage of high-risk areas for PWN, with yellow areas indicating high-risk regions. Guangdong has the highest risk percentage for carbon storage, reaching 29.98%, followed by Guizhou and Guangxi with 6.11% and 9.55%, respectively. The risk in Zhejiang and Liaoning is lower, with percentages of 3.19% and 3.05%, respectively.

Overall, Guangdong faces the greatest forest carbon storage risk, especially in areas with widespread PWN transmission, resulting in the greatest potential for carbon storage loss. Forest carbon storage in Guizhou and Guangxi is also under significant risk, while the risk in Zhejiang and Liaoning is lower. To reduce carbon storage losses, particularly in high-risk areas like Guangdong, Guangxi, and Guizhou, it is essential to strengthen PWN control measures and improve forest management and protection in these regions.

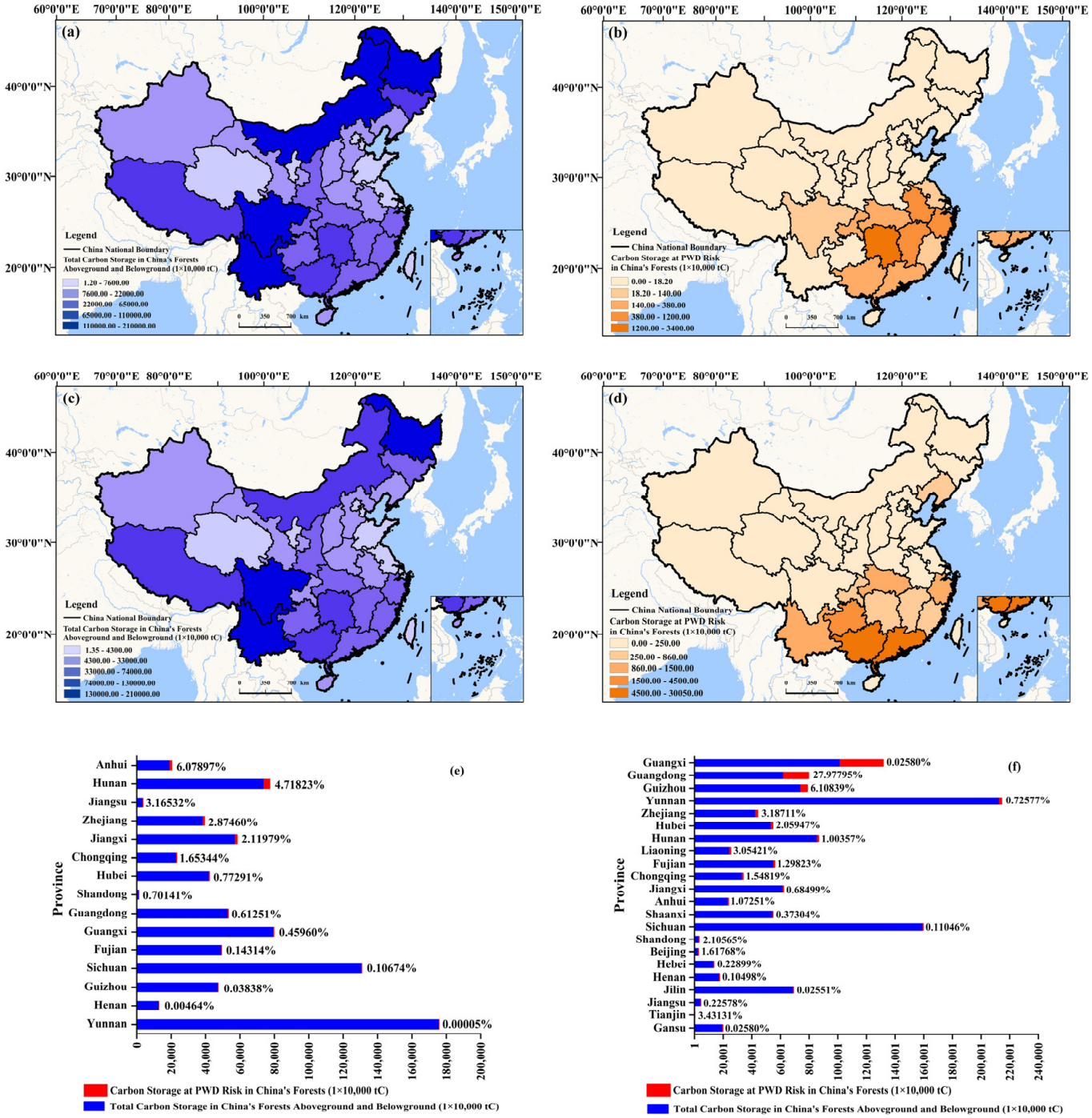


Figure 12. Provincial patterns of total aboveground and belowground forest carbon stocks and risk models in China. (**a**) Total aboveground and belowground forest carbon stocks by province in 2002; (**b**) distribution of forest carbon stock risks across provinces in 2002; (**c**) total aboveground and belowground forest carbon stocks by province in 2021; (**d**) distribution of forest carbon stock risks across provinces in 2021; (**e**) proportion of PWN risk carbon stocks in each province in 2002. Red and blue represent risk carbon stocks and total carbon stocks, respectively; (**f**) proportion of PWN risk carbon stocks in each province in 2021. Red and blue represent risk carbon stocks and total carbon stocks, respectively.

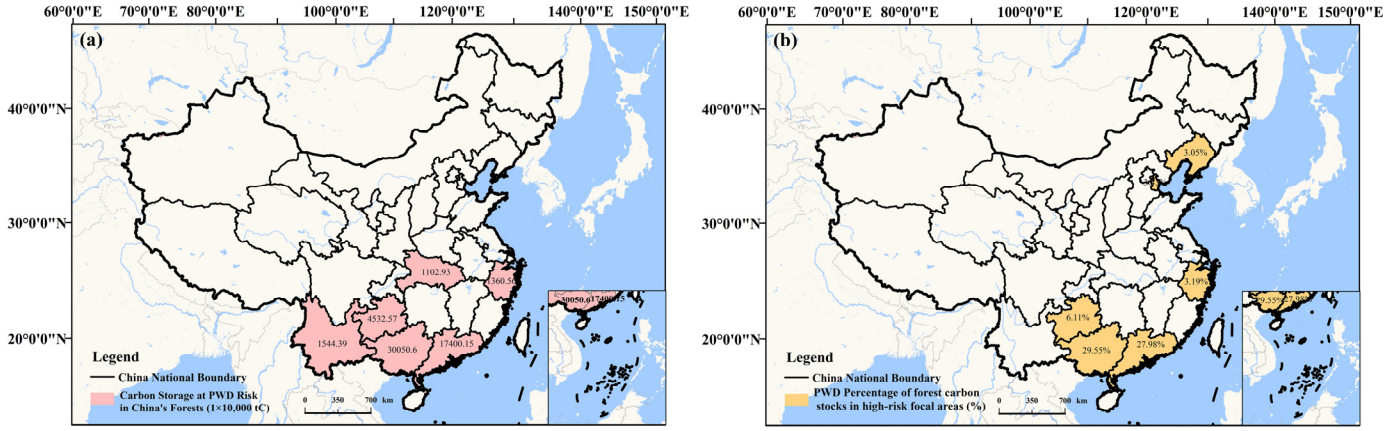


Figure 13. Key risk areas of forest carbon stocks affected by pine wood nematode (PWN) in China in 2021 (tons of carbon per hectare): (**a**) top six provinces by total forest carbon risk; (**b**) top six provinces by percentage of forest carbon risk.

4. Discussion

China has abundant forest resources, with coniferous forest ecosystems, especially those represented by pines, playing a critical role in the country's forest distribution [53]. These forests contribute significantly to carbon sequestration, absorbing and converting atmospheric CO_2 into biomass, which is essential for mitigating climate change, regulating regional climates, and maintaining ecological balance [54]. However, pine wood nematode (PWN)-induced pine wilt disease (PWD) poses a serious threat to China's forest ecosystems.

This study found significant differences in the resistance of various tree species to PWN. Highly sensitive host species, such as Masson pine and Chinese red pine, are primarily found in the humid areas of the eastern and southern regions, while less sensitive species like white pine and larch are distributed in the colder, high-altitude areas of the north and southwest. This distribution pattern reflects the interplay between species adaptability and climate conditions. The concentration of PWN-sensitive species in warm and humid regions increases their vulnerability, exacerbating carbon stock losses in these areas. The distribution and ecological sensitivity of host species directly affect the vulnerability of forest ecosystems. In recent years, the carbon sequestration function of high-sensitivity species has significantly decreased due to PWD outbreaks, further aggravating the carbon source trend of these ecosystems. Therefore, control and restoration measures for areas with high-sensitivity species are critical [55].

Using the R programming language and Kuenm package, this study calibrated and evaluated the key parameters of the MaxEnt model to identify optimal parameter settings, which improved the model's prediction accuracy. The optimized MaxEnt model effectively reduced complexity and improved the fit between predicted results and actual data [56]. Based on this model, we predicted the potential distribution areas of PWN and visually demonstrated the spatial distribution patterns and suitability in China for 2002 and 2021 while quantifying the driving factors of PWN spread through environmental variables.

Although MaxEnt is widely used for species distribution modeling, it has some limitations in specific scenarios. Firstly, the model heavily depends on the distribution data, and biases or uneven distribution of data may affect the accuracy of the predictions [57]. For example, in this study, the PWN distribution points were mainly concentrated in the eastern and southern regions, which may have led to an underestimation of suitability in the central and northern regions. Secondly, the selection and preprocessing of environmental variables significantly impact the model's performance. Despite using Jackknife

and Spearman correlation analysis to select 23 environmental variables, multicollinearity between variables could still pose a problem.

The study further indicates that the key drivers of PWN spread include natural factors (such as altitude, annual temperature, and seasonal precipitation) and human activities (such as population density, land use changes, and transportation networks). In 2002, PWN distribution was primarily controlled by natural factors, particularly altitude and climate conditions, with low-altitude and warm, humid climates being more vulnerable to PWN invasion. However, data from 2021 show that the impact of human activities has significantly increased, particularly in economically developed regions in the eastern and southern parts of China, where transportation networks and land use changes have accelerated the spread of PWD. This result is consistent with existing research, which highlights the growing role of human activities in the spread of invasive species, particularly through the transport of dead wood-carrying pathogens, leading to the spread of the disease to new areas [58,59]. Therefore, future control measures should focus on areas with high human activity, strengthening monitoring and management, and reducing the risks of PWN spread due to human interference.

In response to the dual challenge of PWN invasion, forest protection strategies should focus on enhancing the resilience of forest ecosystems. Specific measures include implementing diversified planting, improving tree species resistance, and using biological control technologies to control the spread of PWN. For high-risk areas, it is important to select more adaptable tree species and avoid over-reliance on monoculture. Additionally, sound forest management and restoration strategies, especially in PWN high-risk regions, can significantly reduce carbon stock losses.

The spatial suitability study of PWN shows that, from 2002 to 2021, the high-suitability area for PWN expanded from 68,000 km^2 to 184,000 km^2, especially in the eastern coastal and southern humid regions. Although China's forest carbon stock increased from 111.34 billion tons of carbon (tC) to 168.05 billion tC, a rise of over 50%, the risk carbon stock affected by PWN also increased from 87 million tC to 99 million tC, posing a continuing threat to the carbon sequestration capacity of forests. This trend aligns with previous studies, demonstrating the widespread destructive impact of invasive pests on global forest carbon balance. According to the 2002 national forest resource survey in China, the forest area was 158.94 million hectares, with a stock of 112.7 billion cubic meters and a total carbon stock of 111.34 billion tC. The latest data show that, by 2024, China's forest area had increased to 34.65 billion mu, with a forest coverage rate of 24.02%, a stock of 194.93 billion cubic meters, and a total carbon stock of 114.43 billion tC. The carbon stock results from 2002 and 2021 in this study closely match the official statistics, confirming the validity and scientific accuracy of the findings [60,61].

Furthermore, the study reveals the varying risk distribution of forest carbon stocks due to PWN invasion across different regions. Guangdong Province accounts for 27.98% of the national carbon stock risk, with significant increases observed in Guizhou, Zhejiang, and Liaoning. The humid climate, dense forest resources, and high human activity levels are the primary reasons these regions have become the high-risk areas for forest carbon stocks in China. However, there are notable differences in the degree of carbon stock risk across different regions. For instance, the eastern coastal regions have relatively concentrated carbon stock losses due to rapid economic development and high human activity, accelerating PWN spread. In contrast, the southwestern and central regions are gradually becoming new risk areas, indicating the inland expansion of PWN's spread. This trend reflects the dynamic disturbance of ecosystems. In the future, differentiated regional control strategies for PWN should be emphasized. For example, strengthening forest monitoring and management, and promptly detecting and addressing PWN invasions,

particularly in high-risk regions, should be prioritized. Furthermore, enhancing forest ecosystem resilience through biodiversity improvement and controlling the spread of invasive species can increase carbon sequestration capacity. Ecological restoration efforts should include protecting and restoring natural forests to boost carbon absorption capacity and mitigate carbon stock losses caused by pests and diseases.

Although the MaxEnt model performs well in predicting the suitable habitats of PWN, its accuracy is still affected by data quality and spatial distribution biases. In this study, the PWN distribution points were concentrated in the eastern and southern regions, which may lead to an underestimation of the suitability in the central and northern regions. Additionally, the MaxEnt model relies on static environmental variables, which may not accurately reflect the impact of future climate change on PWN spread. This study simplified the carbon recovery dynamics and did not fully consider other ecological disturbance factors (such as storms and fires). Therefore, future studies should combine higher-resolution time series data and consider the dynamic changes of climate change and human activities to further optimize the model and improve prediction accuracy. Moreover, model parameter determination still carries uncertainty, especially in the absence of long-term continuous observation data. Future studies should expand the application scenarios of the model, combining high spatial-temporal resolution data to refine simulations of carbon stock dynamics. With the intensification of climate change, it is necessary to conduct in-depth research on the global mechanisms of PWN spread and its long-term impacts on the carbon cycle, while strengthening local and regional control measures to mitigate the threats posed by PWN to China's forest carbon stocks and ecosystems.

5. Conclusions

This study has provided a comprehensive risk assessment of the forest carbon stock loss due to pine wood nematode (PWN) invasion in China, based on an optimized MaxEnt model and multi-source data. The results show that the spread of pine wilt disease (PWD) has significantly accelerated, particularly after 2018, with the number of affected counties rapidly increasing to 615 by 2021. The suitable habitat for PWN has expanded from 68,000 km^2 in 2002 to 184,000 km^2 in 2021, with warm, humid climate conditions and human activities significantly driving its spread. The study also found that regions such as Guangxi, Guangdong, Yunnan, Guizhou, Zhejiang, and Hubei have seen a sharp increase in forest carbon risk, with Guangxi's carbon risk amounting to 15.44 million tons of carbon, accounting for 29.55% of the total forest carbon stock in the province.

The study further reveals significant differences in tree species' sensitivity to PWN. Highly sensitive species, such as Masson's pine and black pine, are concentrated in the southeastern coastal regions, while less sensitive species, such as white pine and larch, exhibit stronger resistance in the northern and southwestern areas. Although China's forest carbon stock has increased from 111.34 billion tons of carbon (tC) in 2002 to 168.05 billion tC in 2021, reflecting the success of ecological restoration and carbon sequestration policies, the carbon risk due to PWN invasion has also increased, from 87 million tC to 99 million tC, highlighting the threat to carbon storage capacity.

To address the threat of PWN invasion to forest carbon stocks, the study emphasizes the necessity of urgent intervention in high-risk areas. This includes strengthening monitoring, regularly assessing the spread of PWN and changes in forest carbon stocks, and responding promptly with remote sensing technology and ground surveys. Additionally, the study recommends enhancing forest management, especially increasing protective measures in affected areas, reducing the felling of pines and human interference, and ensuring the health of ecosystems. The study calls on the government to formulate specific control policies, promote inter-regional coordination and cooperation, establish a joint

control system, strengthen early warning and biological control measures, and support local governments and communities in participating in control efforts. Finally, the study emphasizes the need for all stakeholders to strengthen cooperation, implement control measures effectively, and ensure the health and sustainable development of forest ecosystems, safeguarding forests' role in climate regulation and carbon sequestration and contributing to global climate change mitigation.

Author Contributions: Concept and methodology, W.H. and D.W.; software and verification, S.X.; writing—original manuscript, S.X.; Writing -editing and review, S.X., H.S., J.Y., B.Z., X.M. and J.D. All authors have read and agreed to the published version of the manuscript.

Funding: This research was funded by the National Key R&D Program (2024YFE0198605), the National Natural Science Foundation of China (42201355), the Sino-UK Crop Pest and Disease Forecasting & Management Joint Laboratory, the SINO-EU Dragon 6 Proposal (ID 95250), and GEO-PDRS: Global Vegetation Pest and Disease Dynamic Remote Sensing Monitoring and Forecasting.

Data Availability Statement: The data presented in this study are available from the corresponding authors.

Acknowledgments: The authors sincerely thank Steven J. Phillips's team at Columbia University for developing the Maxent v3.4.4 software. We appreciate Tang Jimin's help with practical work. In addition, Xu Shaoxiong would like to thank Xu Shaohua for his help with typesetting. We would like to thank the reviewers for their helpful and constructive comments, which have improved the paper.

Conflicts of Interest: The authors declare no conflicts of interest.

References

1. Xu, B.; Guo, Z.; Piao, S.; Fang, J. Biomass carbon stocks in China's forests between 2000 and 2050: A prediction based on forest biomass-age relationships. *Sci. China Life Sci.* **2010**, *53*, 776–783. [CrossRef] [PubMed]
2. Fang, J.; Yu, G.; Liu, L.; Hu, S.; Chapin, F.S. Climate change, human impacts, and carbon sequestration in China. *Proc. Natl. Acad. Sci. USA* **2018**, *115*, 4015–4020. [CrossRef] [PubMed]
3. Piao, S.; Yue, C.; Ding, J.; Guo, Z. Perspectives on the role of terrestrial ecosystems in the 'carbon neutrality' strategy. *Sci. China Earth Sci.* **2022**, *65*, 1178–1186. [CrossRef]
4. Masson-Delmotte, V.; Zhai, P.; Pörtner, H.O.; Roberts, D.; Skea, J.; Shukla, P.R.; Pirani, A.; Moufouma-Okia, W.; Péan, C.; Pidcock, R.; et al. Global warming of 1.5 °C. In *An IPCC Special Report on the Impacts of Global Warming of 1.5 °C Above Pre-Industrial Levels and Related Global Greenhouse Gas Emission Pathways, in the Context of Strengthening the Global Response to the Threat of Climate Change, Sustainable Development, and Efforts to Eradicate Poverty*; Cambridge University Press: Cambridge, UK, 2018; pp. 93–174.
5. Wang, W.; Zhu, Q.; He, G.; Liu, X.; Peng, W.; Cai, Y. Impacts of climate change on pine wilt disease outbreaks and associated carbon stock losses. *Agric. For. Meteorol.* **2023**, *334*, 109426. [CrossRef]
6. Kurz, W.A.; Stinson, G.; Rampley, G.J.; Dymond, C.C.; Neilson, E.T. Risk of natural disturbances makes future contribution of Canada's forests to the global carbon cycle highly uncertain. *Proc. Natl. Acad. Sci. USA* **2008**, *105*, 1551–1555. [CrossRef] [PubMed]
7. Liu, Y.; Reich, P.B.; Li, G.; Sun, S. Tree mortality caused by insect outbreak reduces carbon sequestration in temperate forests. *For. Ecol. Manag.* **2011**, *259*, 1522–1530. [CrossRef]
8. Quirion, B.R.; Domke, G.M.; Walters, B.F.; Lovett, G.M.; Fargione, J.E.; Greenwood, L.; Hereof-King, K.; Randall, J.M.; Fei, S. Insect and disease disturbances correlate with reduced carbon sequestration in forests of the contiguous United States. *Front. For. Glob. Change* **2021**, *4*, 716582. [CrossRef]
9. Bright, B.C.; Hicke, J.A.; Hudak, A.T. Estimating aboveground carbon stocks of a forest affected by mountain pine beetle in Idaho using lidar and multispectral imagery. *Remote Sens. Environ.* **2012**, *124*, 270–281. [CrossRef]
10. Gao, R.; Luo, Y.; Wang, Z.; Yu, H.; Shi, J. Patterns of biomass, carbon, and nitrogen storage distribution dynamics after the invasion of pine forests by *Bursaphelenchus xylophilus* (Nematoda: Aphelenchoididae) in the Three Gorges Reservoir Region. *J. For. Res.* **2018**, *29*, 459–470. [CrossRef]
11. Pfeifer, E.M.; Hicke, J.A.; Meddens, A.J. Observations and modeling of above-ground tree carbon stocks and fluxes following a bark beetle outbreak in the western United States. *Glob. Change Biol.* **2011**, *17*, 339–350. [CrossRef]
12. Hunt, S.L.; Newman, J.; Otis, G.W. Threats and Impacts of Exotic Pests Under Climate Change: Implications for Canada's Forest Ecosystems and Carbon Stocks. BIOCAP Canada Foundation. Available online: http://www.biocap.ca/rif/report/Hunt_S.pdf (accessed on 3 February 2025).

13. Tang, X.; Yuan, Y.; Li, X.; Zhang, J. Maximum entropy modeling to predict the impact of climate change on pine wilt disease in China. *Front. Plant Sci.* **2021**, *12*, 764. [CrossRef] [PubMed]
14. Zhao, L.L.; Wei, W.; Kang, L.; Sun, J.H. Chemotaxis of the pinewood nematode, Bursaphelenchus xylophilus, to volatiles associated with host pine, *Pinus massoniana*, and its vector *Monochamus alternatus*. *J. Chem. Ecol.* **2007**, *33*, 1207–1216. [CrossRef]
15. Cardoso, J.M.S.; Manadas, B.; Abrantes, I.; Robertson, L.; Arcos, S.C.; Troya, M.T.; Navas, A.; Fonseca, L. Pine wilt disease: What do we know from proteomics? *BMC Plant Biol.* **2024**, *24*, 98. [CrossRef]
16. Faria, J.M.; Barbosa, P.; Bennett, R.N.; Mota, M.; Figueiredo, A.C. Bioactivity against *Bursaphelenchus xylophilus*: Nematotoxics from essential oils, essential oils fractions, and decoction waters. *Phytochemistry* **2013**, *94*, 220–228. [CrossRef] [PubMed]
17. Yu, L.; Zhan, Z.; Ren, L.; Li, H.; Huang, H.; Luo, Y. Impact of stand-and landscape-level variables on pine wilt disease-caused tree mortality in pine forests. *Pest Manag. Sci.* **2023**, *79*, 1791–1799. [CrossRef] [PubMed]
18. Hao, Z.; Fang, G.; Huang, W.; Ye, H.; Zhang, B.; Li, X. Risk prediction and variable analysis of pine wilt disease by a maximum entropy model. *Forests* **2022**, *13*, 342. [CrossRef]
19. Li, S.; Sun, H.; Zhou, Y.; Li, X.; Yu, Z.; Dong, Z. Occurrence of major forest pests and diseases in China in 2021 and prediction of trends in 2022. *Chin. J. For. Pathol. Entomol.* **2022**, *3*, 1–5. [CrossRef]
20. Hao, Z.; Huang, J.; Zhou, Y.; Fang, G. Spatiotemporal pattern of pine wilt disease in the Yangtze River Basin. *Forests* **2021**, *12*, 731. [CrossRef]
21. Sage, R.F. Global change biology: A primer. *Glob. Change Biol.* **2020**, *26*, 3–30. [CrossRef]
22. Ontl, T.A.; Janowiak, M.K.; Swanston, C.W.; Daley, J.; Handler, S.; Cornett, M.; Hagenbuch, S.; Handrick, C.; McCarthy, L.; Patch, N. Forest management for carbon sequestration and climate adaptation. *J. For.* **2020**, *118*, 86–101. [CrossRef]
23. Yang, D.; Qin, S.; Chi, S.; Sun, D.; Feng, Z.; Guan, Z.; Yu, Z.; Liu, Z.; Li, X.; Liu, C.; et al. Research status and hotspot analysis of pine wood nematode disease based on CiteSpace. *Nat. Protected Areas* **2022**, *2*, 115–128. [CrossRef]
24. Lissovsky, A.A.; Dudov, S.V. Species-distribution modeling: Advantages and limitations of its application. 2. MaxEnt. *Biol. Bull. Rev.* **2021**, *11*, 265–275. [CrossRef]
25. Austin, M.P. Spatial prediction of species distribution: An interface between ecological theory and statistical modelling. *Ecol. Modell.* **2002**, *157*, 101–118. [CrossRef]
26. Elith, J.; Leathwick, J.R. Species distribution models: Ecological explanation and prediction across space and time. *Annu. Rev. Ecol. Evol. Syst.* **2009**, *40*, 677–697. [CrossRef]
27. Booth, T.H.; Nix, H.A.; Busby, J.R.; Hutchinson, M.F. BIOCLIM: The first species distribution modelling package, its early applications and relevance to most current MAXENT studies. *Divers. Distrib.* **2014**, *20*, 1–9. [CrossRef]
28. Komori, O.; Saigusa, Y.; Eguchi, S.; Kubota, Y. Cumulant-based approximation for fast and efficient prediction for species distribution. *arXiv* **2024**, arXiv:2405.14456. [CrossRef]
29. Wang, L.; Jackson, D.A. Effects of sample size, data quality, and species response in environmental space on modeling species distributions. *Landscape Ecol.* **2023**, *38*, 4009–4031. [CrossRef]
30. Fletcher, R.J., Jr.; Hefley, T.J.; Robertson, E.P.; Zuckerberg, B.; McCleery, R.A.; Dorazio, R.M. A practical guide for combining data to model species distributions. *Ecology* **2019**, *100*, e02710. [CrossRef]
31. Yang, L.; Zhu, X.; Song, W.; Shi, X.; Huang, X. Predicting the potential distribution of 12 threatened medicinal plants on the Qinghai-Tibet Plateau, with a maximum entropy model. *Ecol. Evol.* **2024**, *14*, e11042. [CrossRef]
32. Merow, C.; Smith, M.J.; Silander, J.A., Jr. A practical guide to MaxEnt for modeling species' distributions: What it does, and why inputs and settings matter. *Ecography* **2013**, *36*, 1058–1069. [CrossRef]
33. Wang, J.; Deng, J.; Yan, W.; Zheng, Y. Habitat suitability of pine wilt disease in Northeast China under climate change scenario. *Forests* **2023**, *14*, 1687. [CrossRef]
34. Ikegami, M.; Jenkins, T. Estimate global risks of a forest disease under current and future climates using species distribution model and simple thermal model—Pine Wilt disease as a model case. *For. Ecol. Manag.* **2018**, *409*, 343–352. [CrossRef]
35. Zhou, Y.; Ge, X.; Zou, Y.; Guo, S.; Wang, T.; Tao, J.; Zong, S. Prediction of the potential geographical distribution of *Hylurgus ligniperda* at the global scale and in China using the MaxEnt model. *J. Beig. For. Univ.* **2022**, *44*, 90–99. (In Chinese) [CrossRef]
36. Syfert, M.M.; Smith, M.J.; Coomes, D.A. The effects of sampling bias and model complexity on the predictive performance of MaxEnt species distribution models. *PLoS ONE* **2013**, *8*, e55158. [CrossRef]
37. Fourcade, Y.; Engler, J.O.; Rödder, D.; Secondi, J. Map species distributions with MAXENT using a geographically biased sample of presence data: A performance assessment of methods for correcting sampling bias. *PLoS ONE* **2014**, *9*, e97122. [CrossRef] [PubMed]
38. Araújo, M.B.; Guisan, A. Five (or so) challenges for species distribution modelling. *J. Biogeogr.* **2006**, *33*, 1677–1688. [CrossRef]
39. Ji, Y.; Zhou, G.; Luo, T.; Dan, Y.; Zhou, L.; Lv, X. Variation of net primary productivity and its drivers in China's forests during 2000–2018. *For. Ecosyst.* **2020**, *7*, 15. [CrossRef]

40. Luoto, M.; Heikkinen, R.K.; Pöyry, J.; Saarinen, K. Determinants of biogeographical distribution of butterflies in boreal regions. *J. Biogeogr.* **2006**, *33*, 1764–1778. [CrossRef]
41. National Centers for Environmental Information. Global Surface Summary of the Day—GSOD. Version 1.0, NOAA, 1999. Available online: https://www.ncei.noaa.gov/data/global-summary-of-the-day/ (accessed on 3 February 2025).
42. Yang, J.; Huang, X. China 2002 and 2021 30 m Land Cover Dataset. 2021, Earth System Science Data. Available online: https://zenodo.org/records/12779975 (accessed on 3 February 2025).
43. Center for International Earth Science Information Network (CIESIN). Gridded Population of the World, Version 4 (GPWv4): Population Density. *NASA Socioeconomic Data and Applications Center (SEDAC).* 2022. Available online: https://sedac.ciesin.columbia.edu/ (accessed on 3 February 2025).
44. Institute for Environmental Studies (IVM). Global Roads Inventory Project (GRIP): Global Road Density Dataset. GLOBIO. 2020. Available online: https://www.globio.info/ (accessed on 3 February 2025).
45. Quan, Q.; Wu, Y. Integrating Entropy Weight and MaxEnt Models for Ecotourism Suitability Assessment in Northeast China Tiger and Leopard National Park. *Land* **2024**, *13*, 1269. [CrossRef]
46. Zhang, X.; Sun, S.; Yong, S.; Zhou, Z.; Wang, R. *The Vegetation Map of the People's Republic of China (1:1,000,000)*; Science Press: Beijing, China, 2007.
47. CASEarth. The 1:500,000 New Generation Dataset on Vegetation Types of China. Available online: https://www.bio-one.org.cn (accessed on 3 February 2025).
48. National Tibetan Plateau Data Center (TPDC). Dataset of Above- and Below-Ground Vegetation Carbon Stocks in China's Forests (2002–2021). Available online: http://data.tpdc.ac.cn (accessed on 3 February 2025).
49. Zhao, H.; Xian, X.; Yang, N.; Guo, J.; Zhao, L.; Shi, J.; Liu, W.-X. Risk assessment framework for pine wilt disease: Estimating the introduction pathways and multispecies interactions among the pine wood nematode, its insect vectors, and hosts in China. *Sci. Total Environ.* **2023**, *905*, 167075. [CrossRef] [PubMed]
50. Zeng, Y.; Low, B.W.; Yeo, D.C. Novel methods to select environmental variables in MaxEnt: A case study using invasive crayfish. *Ecol. Model.* **2016**, *341*, 5–13. [CrossRef]
51. Li, Z.; Liu, Y.; Zeng, H. Application of the MaxEnt model in improving the accuracy of ecological red line identification: A case study of Zhanjiang, China. *Ecol. Indic.* **2022**, *137*, 108767. [CrossRef]
52. Renner, I.W.; Warton, D.I. Equivalence of MAXENT and Poisson point process models for species distribution modeling in ecology. *Biometrics* **2013**, *69*, 274–281. [CrossRef] [PubMed]
53. Bretthorst, G.L. The maximum entropy method of moments and Bayesian probability theory. *AIP Conf. Proc.* **2013**, *1553*, 3–15. [CrossRef]
54. Luo, Y.; Wang, X.; Zhang, X.; Ren, Y.; Poorter, H. Variation in biomass expansion factors for China's forests in relation to forest type, climate, and stand development. *Ann. For. Sci.* **2013**, *70*, 589–599. [CrossRef]
55. Dsouza, K.B.; Ofosu, E.; Salkeld, J.; Boudreault, R.; Moreno-Cruz, J.; Leonenko, Y. Assessing the climate benefits of afforestation: Phenomenology, processes, methods. *arXiv* **2024**, arXiv:2407.14617. [CrossRef]
56. Hu, B.; Huang, W.; Hao, Z.; Guo, J.; Huang, Y.; Cheng, X.; Zhang, B. Invasion of Pine Wilt Disease: A threat to forest carbon storage in China. *Ecol. Indic.* **2024**, *169*, 112819. [CrossRef]
57. Cobos, M.E.; Peterson, A.T.; Barve, N.; Osorio-Olvera, L. kuenm: An R package for detailed development of ecological niche models using Maxent. *PeerJ* **2019**, *7*, e6281. [CrossRef] [PubMed]
58. Phillips, S.J.; Anderson, R.P.; Schapire, R.E. Maximum entropy modeling of species geographic distributions. *Ecol. Model.* **2006**, *190*, 231–259. [CrossRef]
59. Isbell, F.; Gonzalez, A.; Loreau, M.; Cowles, J.; Diaz, S.; Hector, A.; Turnbull, L.A. Linking the influence and dependence of people on biodiversity across scales. *Nature* **2017**, *546*, 65–72. [CrossRef]
60. Klapwijk, M.J.; Hopkins, A.J.; Eriksson, L.; Pettersson, M.; Schroeder, M.; Lindelöw, Å.; Björkman, C. Reducing the risk of invasive forest pests and pathogens: Combining legislation, targeted management and public awareness. *AMBIO* **2016**, *45* (Suppl. S2), 223–234. [CrossRef] [PubMed]
61. Cheng, K.; Yang, H.; Guan, H.; Ren, Y.; Chen, Y.; Chen, M.; Yang, Z.; Lin, D.; Liu, W.; Xu, J.; et al. Unveiling China's natural and planted forest spatial-temporal dynamics from 1990 to 2020. *ISPRS J. Photogramm. Remote Sens.* **2024**, *209*, 37–50. [CrossRef]

Disclaimer/Publisher's Note: The statements, opinions and data contained in all publications are solely those of the individual author(s) and contributor(s) and not of MDPI and/or the editor(s). MDPI and/or the editor(s) disclaim responsibility for any injury to people or property resulting from any ideas, methods, instructions or products referred to in the content.